Ensemble uncertainty of inherent optical properties

Mhd. Suhyb Salama,[1,*] **Frederic Mélin,**[2] **and Rogier Van der Velde**[1]

[1]*Department of Water Resources, ITC, University of Twente, Hengelosestraat 99, 7500 AA Enschede, The Netherlands*

[2] *Institute for Environment and Sustainability, Joint Research Centre European Commission, 21027 Ispra, Italy*

salama@itc.nl

Abstract: We present a method to evaluate the combined accuracy of ocean color models and the parameterizations of inherent optical proprieties (IOPs), or model-parametrization setup. The method estimates the ensemble (collective) uncertainty of derived IOPs relative to the radiometric error and is directly applicable to ocean color products without the need for inversion. Validation shows a very good fit between derived and known values for synthetic data, with $R^2 > 0.95$ and mean absolute difference (MADi) <0.25 m^{-1}. Due to the influence of observation errors, these values deteriorate to $0.45 < R^2 < 0.5$ and $0.65 <$ MADi < 0.9 for *in-situ* and ocean color matchup data. The method is also used to estimate the maximum accuracy that could be achieved by a specific model-parametrization setup, which represents the optimum accuracy that should be targeted when deriving IOPs. Application to time series of ocean color global products collected between 1997-2007 shows few areas with increasing annual trends of ensemble uncertainty, up to 8 sr m^{-1}decade^{-1}. This value is translated to an error of 0.04 m^{-1}decade^{-1} in the sum of derived absorption and backscattering coefficients at the blue wavelength 440 nm. As such, the developed method can be used as a tool for assessing the reliability of model-parametrization setups for specific biophysical conditions and for identifying hot-spots for which the model-parametrization setup should be reconsidered.

OCIS codes: (010.4450) Oceanic optics; (010.7340) Water.

References and links

1. Z. Su, R. A. Roebeling, J. Schulz, I. Holleman, V. Levizzani, W. J. Timmermans, H. Rott, N. Mognard-Campbell, R. de Jeu, W. Wagner, M. Rodell, M. S. Salama, G. Parodi, and L. Wang, "Observation of Hydrological Processes Using Remote Sensing," in *Treatise on Water Science*, P. Wilderer, ed. (Academic Press, 2011).
2. F. Mélin, "Global distribution of the random uncertainty associated with satellite-derived chla," IEEE Geosci. Remote Sens. Lett. **7**, 220–224 (2010).
3. T. S. Moore, J. W. Campbell, and M. D. Dowell, "A class-based approach to characterizing and mapping the uncertainty of the MODIS ocean chlorophyll product," Remote Sens. Environ. **113**, 2424–2430 (2009).
4. P. Wang, E. Boss, and C. Roesler, "Uncertainties of inherent optical properties obtained from semianalytical inversions of ocean color," Appl. Opt. **44**, 4074–4084 (2005).
5. S. Maritorena and D. Siegel, "Consistent merging of satellite ocean color data sets using a bio-optical model," Remote Sens. Environ. **94**, 429–440 (2005).
6. M. S. Salama, A. G. Dekker, Z. Su, C. M. Mannaerts, and W. Verhoef, "Deriving inherent optical properties and associated inversion-uncertainties in the dutch lakes," Hydrol. Earth Syst. Sci. **13**, 1113–1121 (2009).

#146504 - $15.00 USD Received 25 Apr 2011; revised 4 Jul 2011; accepted 2 Aug 2011; published 15 Aug 2011

7. Z. Lee, R. Arnone, C. Hu, J. Werdell, and B. Lubac, "Uncertainties of optical parameters and their propagations in an analytical ocean color inversion algorithm," Appl. Opt. **49**, 369–381 (2010).
8. M. S. Salama and A. Stein, "Error decomposition and estimation of inherent optical properties," Appl. Opt. **48**, 4926–4962 (2009).
9. Z. Lee, "Remote sensing of inherent optical properties: Fundamentals, tests of algorithms, and applications," Tech. Rep. 5, International Ocean-Colour Coordinating Group (2006).
10. J. Werdell and S. Bailey, "An improved in-situ bio-optical data set for ocean color algorithm development and satellite data product validation," Remote Sens. Environ. **98**, 122–140 (2005).
11. J. G. Acker and G. Leptoukh, "Online analysis enhances use of NASA earth science data," Eos, Trans. AGU **88**, 14–17 (2005).
12. S. Maritorena, D. Siegel, and A. Peterson, "Optimization of a semianalytical ocean color model for global-scale applications," Appl. Opt. **41**, 2705–2714 (2002).
13. H. Gordon, O. Brown, R. Evans, J. Brown, R. Smith, K. Baker, and D. Clark, "A semianalytical radiance model of ocean color," J. Geophys. Res. **93**, 10909–10924 (1988).
14. M. S. Salama and F. Shen, "Stochastic inversion of ocean color data using the cross-entropy method," Opt. Express **18**, 479–499 (2010).
15. Z. Lee, K. Carder, C. Mobley, R. Steward, and J. Patch, "Hyperspectral remote sensing for shallow waters: 2. deriving bottom depths and water properties by optimization," Appl. Opt. **38**, 3831–3843 (1999).
16. A. Bricaud, A. Morel, and L. Prieur, "Absorption by dissolved organic-matter of the sea (yellow substance) in the UV and visible domains," Limnol. Oceanogr. **26**, 43–53 (1981).
17. O. Kopelevich, "Small-parameter model of optical properties of sea waters," in "Ocean Optics," , vol. 1 Physical Ocean Optics, A. Monin, ed. (Nauka, 1983), pp. 208–234.
18. F. Mélin, G. Zibordi and JF. Berthon, "Assessment of satellite ocean color products at a coastal site," Remote Sens. Environ. **110**, 192–215 (2007).
19. E. Laws, *Mathematical Methods for Oceanographers: An Introduction* (John Wiley and Sons, 1997).
20. C. J. Willmott and K. Matsuura, "Advantages of the mean absolute error (MAE) over the root mean square error (RMSE) in assessing average model performance," Climate Res. **30**, 79–82 (2005).
21. M. Salama and Z. Su, "Bayesian model for matching the radiometric measurements of aerospace and field ocean color sensors," Sensors **10**, 7561–7575 (2010).
22. M. S. Salama and Z. Su, "Resolving the subscale spatial variability of apparent and inherent optical properties in ocean color matchup sites," IEEE Trans. Geosci. Remote Sens. **49**, 2612–2622 (2011).
23. M. S. Salama, J. Monbaliu, and P. Coppin, "Atmospheric correction of advanced very high resolution radiometer imagery," Int. J. Remote Sens. **25**, 1349–1355 (2004).
24. M. S. Salama and F. Shen, "Simultaneous atmospheric correction and quantification of suspended particulate matters from orbital and geostationary earth observation sensors," Estuarine Coastal Shelf Sci. **86**, 499–511 (2010).
25. E. Aas, "Estimates of radiance reflected towards the zenith at the surface of the sea," Ocean Sci. **6**, 861-876, (2010)

1. Introduction

Deriving inherent optical properties (IOPs) from ocean color data requires accurate atmospheric correction, reliable retrieval algorithms and a consistent method for uncertainty estimation [1]. Commonly, a subset of the IOPs is retrieved from ocean color data, namely the absorption and backscattering coefficients of the water upper mixed layer. These bulk optical quantities are then related to biophysical characteristics of suspended and dissolved materials in the water. The choice of the retrieval algorithm and IOP parameterizations influences the accuracy of derived IOPs (backscattering and absorption coefficients). Consequently, quantifying the combined effect of both model and parametrization uncertainty on the accuracy of derived IOPs supports the assessment of ocean-color models and facilitates the design of future ocean color retrieval algorithms and IOP parameterizations.

Various methods have been developed to evaluate the uncertainty of derived IOPs. Mélin [2] estimated the uncertainty embedded within chlorophyll-a (chl*a*) concentrations derived from Sea viewing Wide Field-of-view Sensor (SeaWiFS) and Moderate Resolution Imaging Spectroradiometer (MODIS) measurements. Moore *et al.* [3] quantified the uncertainty of Chl*a* concentrations derived from MODIS based on a fuzzy-logic approach to define memberships to specific optical water types. Other studies [4–7] have employed gradient-based methods to

#146504 - $15.00 USD Received 25 Apr 2011; revised 4 Jul 2011; accepted 2 Aug 2011; published 15 Aug 2011

evaluate IOP uncertainties via application of a specific ocean color model, utilizing model derivatives and the difference between model best-fit and observed radiances. Alternatively, Salama and Stein [8] developed a non-gradient based method to quantify and separate uncertainty sources within derived IOPs based on a prior estimate of the radiometric uncertainties and their propagation through the retrievals. However, they also showed that the gradient based method has two inherent limitations: it produces uncertainty values that are proportional to the magnitude of derived IOPs, and it cannot handle radiometric residuals resulting from sensor noise and atmospheric correction.

The uncertainties in derived IOPs are determined by radiometric uncertainties, imperfection in the forward ocean color model and the adopted parametrization. The effect of the used ocean color model and set of parameterizations, or model-parametrization setup on the accuracy of retrieved IOPs has, so far, not been quantified in a single measure. In this paper, we present a method that quantifies the uncertainty of IOPs that follows from a model-parametrization setup. As such, the method provides a single measure of ensemble (collective) uncertainty of IOPs and avoids computing the radiometric uncertainty.

Our method is validated using three data sets. The first is a set of radiative transfer simulations of synthetic IOPs obtained from the International Ocean Color Coordination Group (IOCCG), report-5 [9, IOCCG data set]. The second is *in-situ* measured data of water-leaving radiance and IOPs obtained from the NASA bio-Optical Marine Algorithm Data set (NOMAD), Version 2.a [10, NOMAD data set]. The third consists of concurrent SeaWiFS observations and NOMAD measured inherent and apparent optical properties, Version 1.3 [10, SeaWiFS matchup data set]. Finally, the operational application of the method is demonstrated using time series of IOPs derived from SeaWiFS monthly acquisitions from 1997 to 2007 [11]. From hereon, we assume the difference between known and derived IOPs per unit of radiometric error is equivalent to the uncertainty.

2. Method

2.1. Ensemble Uncertainty of IOPs

Inversion of ocean color models is used to derive IOPs from radiometric observations of water surfaces. These models are based on: (i) approximations that link remote sensing reflectance just above the water surface, $Rs_{\mathrm{w}}(\lambda)$, to the IOPs (generally absorption and backscattering coefficients); (ii) parameterizations of the IOPs as functions of their values at a reference wavelength λ_0. So we have: $Rs_{\mathrm{w}}(\lambda) = f(\mathbf{iop})$, with λ being the wavelength and **iop** being the set of derived IOPs at the reference wavelength λ_0: $\mathbf{iop} = [iop_{i=1}, ..., iop_{i=n}]$. As such, the radiometric uncertainty is propagated towards the derived IOPs as follows,

$$\Delta Rs_{\mathrm{w}}(\lambda) = \sum_{i=1}^{i=n} w_{\mathrm{i}}(\lambda)\Delta iop_i(\lambda_0) + \delta(\lambda), \tag{1}$$

where $\Delta Rs_{\mathrm{w}}(\lambda)$ and $\Delta iop_i(\lambda_0)$ represent the infinitesimal-change in $Rs_{\mathrm{w}}(\lambda)$ and i*th* IOP at the reference wavelength λ_0, $iop_i(\lambda_0)$, respectively; w_i is the partial derivative of remote sensing reflectance with respect to i*th* IOP; i.e. $w_i = \partial Rs_{\mathrm{w}}(\lambda)/\partial iop_i(\lambda_0)$. The term $\delta(\lambda)$ is an error component that represents the accuracy of the used forward ocean color model in describing the relationship between apparent and inherent optical properties. To simplify the mathematical derivations, the term $\delta(\lambda)$ will be imbedded in $\Delta Rs_{\mathrm{w}}(\lambda)$ and its spectral dependence will be dropped.

Equation (1) facilitates estimating the uncertainties of all IOPs if $\Delta Rs_{\mathrm{w}}(\lambda)$ is provided for at least *n* wavelengths, with *n* being the number of derived IOPs which requires prior knowledge on the magnitude of $\Delta Rs_{\mathrm{w}}(\lambda)$. It is, therefore, more convenient to evaluate the uncertainty of

#146504 - $15.00 USD Received 25 Apr 2011; revised 4 Jul 2011; accepted 2 Aug 2011; published 15 Aug 2011

IOPs with respect to $\Delta Rs_{\mathrm{w}}(\lambda)$. We divide both sides of Eq. (1) by $\Delta Rs_{\mathrm{w}}(\lambda)$, and denote the ratio $\Delta iop_i(\lambda_0)/\Delta Rs_{\mathrm{w}}(\lambda)$ as $\phi_i(\lambda)$, we have: $\sum w_i(\lambda)\phi_i(\lambda) = 1$. Dividing both sides by $\sum w_i^2$, yields the collective uncertainty of derived IOPs per unit of radiometric error:

$$\Phi(\lambda) = \sum_{i=1}^{i=n} w_i(\lambda)\phi_i(\lambda) / \sum_{i=1}^{i=n} w_i(\lambda) = 1 / \sum_{i=1}^{i=n} w_i(\lambda). \tag{2}$$

The term $\Phi(\lambda)$ in Eq. (2) is referred to as the ensemble uncertainty of IOPs and can be expressed as,

$$\Phi(\lambda) = \frac{\langle \Delta \mathbf{iop}(\lambda) \rangle}{\Delta Rs_{\mathrm{w}}(\lambda)}, \tag{3}$$

where $\langle \Delta \mathbf{iop}(\lambda) \rangle$ is the weighted sum of IOPs errors, with the i*th* weight being the ratio $w_i(\lambda)/\sum w_i(\lambda)$.

Assuming that the IOPs are mutually independent, we have from the Taylor series approximation of the second moment:

$$\sigma_{\mathrm{r}}^2(\lambda) = \sum_{i=1}^{i=n} w_i^2(\lambda)\sigma_i^2(\lambda_0) + \delta^2 + \ell, \tag{4}$$

where $\sigma_{\mathrm{r}}^2(\lambda)$ is the radiometric variance and $\sigma_i^2(\lambda_0)$ is the variance of the i*th* IOP at the reference wavelength λ_0; δ^2 is an error component analogous to δ in Eq. (1); ℓ represents the covariance terms in the Taylor series expansion. Assuming that the water observed-radiance is governed by independently varying IOPs, gives $\ell \approx 0$. For now, the term δ^2 is embedded in $\sigma_{\mathrm{r}}^2(\lambda)$ for the following steps, but is further elaborated on in the analysis and discussion. Dividing both sides of Eq. (4) by the radiometric variance term yields,

$$\sum_{i=1}^{i=n} w_i^2(\lambda)\psi_i^2(\lambda) = 1, \tag{5}$$

with $\psi_i^2(\lambda) = \sigma_i^2(\lambda_0)/\sigma_{\mathrm{r}}^2(\lambda)$. The ensemble uncertainty of IOPs per radiometric error, $\Psi(\lambda)$, is derived from Eq. (5) by normalizing both sides by the squared sum of partial derivatives and taking its square-root:

$$\Psi(\lambda) = \left(\sum_{i=1}^{i=n} w_i^2(\lambda)\psi_i^2(\lambda) / \sum_{i=1}^{i=n} w_i^2(\lambda) \right)^{0.5} = \left(\sum_{i=1}^{i=n} w_i^2(\lambda) \right)^{-0.5}. \tag{6}$$

Both, $\Phi(\lambda)$ and $\Psi(\lambda)$ represent the ensemble uncertainty of IOPs per unit error of remote sensing reflectance and have the unit of sr m^{-1}. Since underestimation of the absorption coefficient is generally associated with overestimation of the backscattering and vice versa, $\Phi(\lambda)$ is expected to be smaller than the individual uncertainties of absorption and backscattering coefficients. In other words, the under/overestimations cancel each other out. Conversely, $\Psi(\lambda)$ is additive; errors always add up. From hereon, $\Psi(\lambda)$ will be used as the measure of uncertainty instead of $\Phi(\lambda)$.

2.2. Relative Measure of Uncertainty

From the definition of $\Psi(\lambda)$, Eq. (6) can be rewritten as,

$$\Psi(\lambda) = \langle \sigma_{\mathrm{iop}}(\lambda) \rangle / \sigma_r(\lambda), \tag{7}$$

#146504 - $15.00 USD Received 25 Apr 2011; revised 4 Jul 2011; accepted 2 Aug 2011; published 15 Aug 2011

where $\langle \sigma_{\rm iop}(\lambda_0) \rangle$ is the sum of weighted IOPs uncertainties:

$$\langle \sigma_{\rm iop}(\lambda) \rangle = \left(\frac{\sum w_i^2(\lambda) \sigma_i^2(\lambda_0)}{\sum w_i^2(\lambda)} \right)^{0.5} = \sigma_{\rm r}(\lambda) \left(\sum_{i=1}^{i=n} w_i^2(\lambda) \right)^{-0.5}. \quad (8)$$

Dividing both sides of Eq. (7) by the sum of derived IOPs, $cb_{\rm d}(\lambda) = \sum iop_i(\lambda)$, we have

$$\Psi^{\rm N}(\lambda) = \frac{\rm CV(\lambda)}{\sigma_r(\lambda)} = \frac{\Psi(\lambda)}{cb_{\rm d}(\lambda)}, \quad (9)$$

where the parameter $\rm CV(\lambda)$ is the ratio, $\rm CV(\lambda) = \langle \sigma_{\rm iop}(\lambda) \rangle / cb_{\rm d}(\lambda)$. The ratio, $\Psi^{\rm N}(\lambda)$, in Eq. (9) is a measure of the relative ensemble uncertainty per radiometric error and has units of sr. The reciprocal of Eq. (9) is a measure of the radiometric uncertainty with respect to $\rm CV(\lambda)$,

$$\sigma_{\rm r}^{\rm N}(\lambda) = \frac{\sigma_r(\lambda)}{\rm CV(\lambda)} = \frac{cb_{\rm d}(\lambda)}{\Psi(\lambda)}. \quad (10)$$

$\sigma_{\rm r}^{\rm N}(\lambda)$ in Eq. (10) is called the normalized radiometric uncertainty, and quantifies the radiometric uncertainty per unit of relative error of IOPs with the $\rm sr^{-1}$ unit.

3. Used Data Sets and Ocean Color Model

Four data sets are used in this study, three to validate the proposed method and one to demonstrate its potential for assessing global ocean color products. The validation data include simulated, *in-situ* measured and ocean color matchup data. Simulated data are radiative transfer simulations with the synthetic IOPs [9, IOCCG data set] as input, performed for a 30° sun zenith over the 400 nm to 720 nm spectral range with 10 nm interval. Inelastic scattering, such as Raman scattering, chlorophyll fluorescence etc, were excluded from the simulations. *In-situ* measured data of water-leaving radiance and IOPs are taken from the NOMAD data set, Version 2.a [10, NOMAD data set]. Ocean color matchup data are concurrent SeaWiFS observations and NOMAD measured inherent and apparent optical properties, Version 1.3 [10, SeaWiFS matchup data set]. Information on the different versions of NOMAD data sets can be found on SeaWiFS Bio-optical Archive and Storage System (SeaBASS): `http://seabass.gsfc.nasa.gov/seabasscgi/nomad.cgi`. Global ocean color products of monthly IOPs data are downloaded from the Goddard Earth Sciences Data and Information Services Center, Interactive Online Visualization and Analysis Infrastructure (Giovanni) [11] and covered the period between 1997 and 2007. This set includes SeaWiFS monthly products of IOPs derived from the Garver-Siegel-Maritorena (GSM) [12] model-parametrization setup.

The GSM model is used to relate the IOPs to the radiometric quantities of ocean color data as [12, 13],

$$Rs_{\rm w}(\lambda) = t^2/n^2 \sum_{i=1}^{i=2} g_i u^i(\lambda), \quad (11)$$

where t is the transmission function from water to air and taken equal to $t = 0.95$ for the nadir viewing angle; n is the water index of refraction and is taken equal to 1.334; g_i are model expansion parameters, for which $g_1 = 0.0949$ and $g_2 = 0.0794$ are adopted [12, 13]; and $u(\lambda)$ is the ratio $b_b(\lambda)/(a(\lambda)+b_b(\lambda))$, with $a(\lambda)$ and $b_b(\lambda)$ as the bulk absorption and the backscattering coefficients of the water upper layer, respectively. Three IOPs will be considered at the reference wavelength $\lambda_0 = 440$ nm: the absorption of chlorophyll-a (Chl*a*), $a_{\rm chl}a(440)$, the lumped absorption effect of detritus and gelbstoff, $a_{\rm dg}(440)$ and the backscattering of suspended particulate matter (SPM), $b_{b\rm p}(440)$. The parameterizations of Salama *et al.* [6, 14] are used for

#146504 - $15.00 USD Received 25 Apr 2011; revised 4 Jul 2011; accepted 2 Aug 2011; published 15 Aug 2011

simulated, *in-situ* measured and SeaWiFS matchup data. For global ocean color products of IOPs, however, the original parameterizations of the GSM model [12] are applied. The difference between these two parameterizations is only in the expression of $a_{\mathrm{chl}a}(\lambda)$ at the reference wavelength λ_0.

We present an application of our method to the existing global products (SeaWiFS) to demonstrate its potential for evaluating the uncertainty of existing model-parametrization setups. In this context, slight differences in the model-parameterizations setup will not affect the conclusions of this application. Parameterizations of IOPs with respect to the reference wavelength $\lambda_0 = 440$ nm are as follows: the coefficient $a_{\mathrm{chl}a}(\lambda)$ is obtained from [15]: $a_{\mathrm{ph}}(\lambda) = a_{\mathrm{ph}}(440)[a_0(\lambda) + a_1(\lambda)\log a_{\mathrm{ph}}(440)]$ with a_0 and a_1 tabulated; the coefficient $a_{\mathrm{dg}}(\lambda)$ is defined as in [16]: $a_{\mathrm{dg}}(\lambda) = a_{\mathrm{dg}}(440)\zeta_{\mathrm{dg}}$, where $\zeta_{\mathrm{dg}} = \exp[-s(\lambda - 440)]$ describes the spectral shape via $s = 0.021$ nm^{-1}; the SPM backscattering coefficient is parameterized as in [17]: $b_{b\mathrm{spm}}(\lambda) = b_{b\mathrm{spm}}(440)\zeta_{\mathrm{spm}}$, in which $\zeta_{\mathrm{spm}} = (440 \cdot \lambda^{-1})^y$ describes the spectral dependency with $y = 1.1$.

4. Validation

The cross-entropy method of Salama [14] is used to derive the IOPs from radiometric measurements. The partial derivatives, w_i, of Eq. (11) are computed with respect to the derived IOPs. The ensemble uncertainty is derived from Eq. (6) as derived_error $= \Psi(\lambda)\sigma_{\mathrm{r}}(\lambda)$. The radiometric uncertainty, $\sigma_{\mathrm{r}}^2(\lambda)$, is computed as $(x_{\mathrm{d}} - x_{\mathrm{k}})^2$ with x being the reflectance. The quantity, x_{d}, is the best-fit spectrum derived from inverting Eq. (11), whereas x_{k} refers to the known reflectance, in this case from the IOCCG-simulated or NOMAD-measured spectra. For the SeaWiFS-matchup set, these two quantities (x_{d} and x_{k}) are replaced by *in-situ* measured and satellite observed spectra, respectively. The known values of ensemble-uncertainties are estimated as,

$$\mathrm{known\_error}^2(\lambda) = \left(\sum w_i^{*2}(\lambda)\Delta iop_i^2(\lambda_0) + \delta^2\right) / \sum w_i^{*2}(\lambda), \tag{12}$$

where Δiop_i is the difference between the derived and measured i*th* IOPs, and w_i^* is the i*th* partial derivatives computed using the measured values of IOPs. The error parameter, δ^2, is estimated as $\delta^2 = (x_{\mathrm{m}} - x_{\mathrm{k}})^2$, in which x_{m} is the output of Eq. (11) using the measured IOPs and x_{k} is the observed (or known) spectra (e.g. IOCCG-simulated, NOMAD-measured or SeaWiFS-observed).

The NOMAD data subset is selected such that each site has radiometric observations and three IOPs measurements, $a_{\mathrm{chl}a}(440)$, $a_{\mathrm{dg}}(440)$ and $b_{b\mathrm{p}}(440)$. On the other hand, the SeaWiFS-matchup subset is composed such that each site has radiometric observations and at least two measured absorption coefficients, $a_{\mathrm{chl}a}(440)$ and $a_{\mathrm{dg}}(440)$. Missing measurements of $b_{b\mathrm{p}}(440)$ in the SeaWiFS-matchup subset are substituted by their estimates as derived from the measured spectra. This is justified by studies showing that the uncertainties associated with the derivation of the backscattering coefficient, $b_{b\mathrm{p}}(440)$, are much lower than those found for absorption [9, 18]. In total, there are 90 NOMAD and 123 SeaWiFS-matchup sites satisfying this criterion.

Derived and known values for the wavelength 440 nm are log-transformed and compared in Fig. 1 for the three data sets.

The fits between derived and known uncertainties in Fig. 1 are assessed using three goodness-of-fit parameters:
i- R^2, coefficient of determination;
ii- MADi, mean absolute differences between derived values and the regression line;
iii- RMSE, root mean of squared error.
The regression line was computed using type-II model [19] and following the practice of the IOCCG report [9]. The goodness-of-fit parameters are computed for each data set separately as well as for all data points and are given in Table 1.

#146504 - $15.00 USD Received 25 Apr 2011; revised 4 Jul 2011; accepted 2 Aug 2011; published 15 Aug 2011

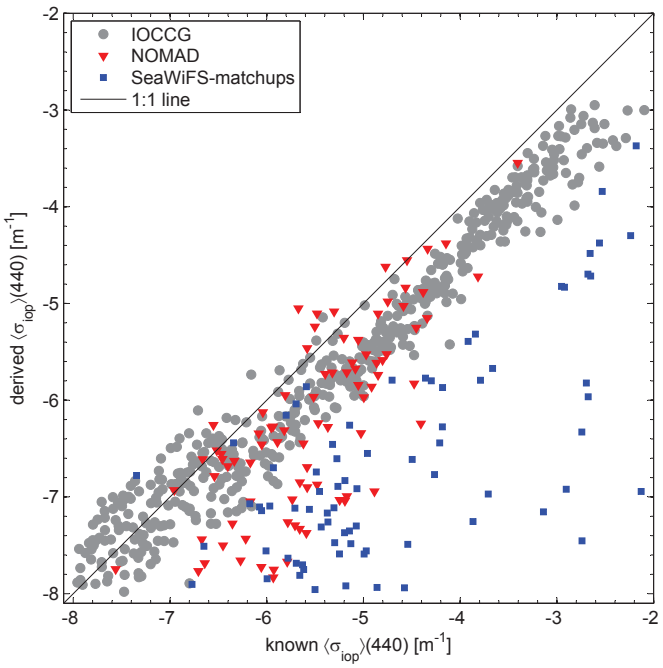

Fig. 1. Known versus estimated ensemble-uncertainties at 440 nm expressed in m^{-1}, of derived IOPs from the three data sets of (a) : IOCCG, gray circles ; (b): NOMAD, red triangles and; (c) : SeaWiFS-matchup in blue squares. The values are log transformed.

Figure 1 and Table 1 show that derived and known uncertainty values have a good linear relationship, with MADi and RMSE values ranging from minima for IOCCG to maxima for SeaWiFS-matchup. Correspondingly, the values of R^2 decrease from about 0.96 for IOCCG to 0.50 for NOMAD and reaches 0.45 for SeaWiFS-matchup. Table 1 and Fig. 1 confirm that the proposed method produces acceptable estimates of uncertainty for the three data sets. Overall, the simulated, measured and ocean color matchup yield a $R^2 \sim 0.61$, MADi < 0.7 and RMSE < 1.2.

5. Discussions

5.1. Formulation

The error term, δ^2, was included in Eq. (4) to account for the uncertainty of the forward model. Figure 2 shows the comparison of σ_r^2 on the X-axis, computed as $(x_d - x_k)^2$, against Eq. (4) on the Y-axis, with δ included (red dots) and without δ (grey circles). This figure is produced

Table 1. Goodness-of-Fit Parameters between Known and Derived Ensemble Uncertainties at 440 nm Using the Three Data Sets

Data set	n	R^2	MADi	RMSE
IOCCG	500	0.955	0.235	0.507
NOMAD	90	0.498	0.654	1.110
SeaWiFS-matchup	123	0.446	0.879	2.627
Total	713	0.609	0.674	1.228

#146504 - $15.00 USD Received 25 Apr 2011; revised 4 Jul 2011; accepted 2 Aug 2011; published 15 Aug 2011

using the IOCCG data set and serves as a reference.

The best-fit parameters, R^2, MADi and RMSE, between known and derived radiometric uncertainties and the effect of including δ are shown in Table 2. It is obvious from Fig. 2 and Table 2 that adding δ improves the results for all wavelengths, with 13-35 % increase in R^2 and 13-44% decrease in MADi. The same improvement in RMSE is, however, more difficult to note. This can be attributed to the nature of RMSE which depends, apart from accuracy, also on the distribution of errors [20]. Willmot and Matsuura [20] recommend using mean absolute error (MADi in this study) instead of RMSE.

Recall that the following approximations were used: $\delta^2 = (x_m - x_k)^2$ and $\sigma_r^2 = (x_d - x_k)^2$, from which the following relation can be derived $\delta^2 = \sigma_r^2 + x_m^2 - x_d^2 + 2x_k(x_d - x_m)$. Substituting δ in Eq. (4) gives $\sum w_i^2 \sigma_i^2 = x_d^2 - x_m^2 + 2x_k(x_m - x_d)$. For this to hold, i.e. $\sum w_i^2 \sigma_i^2 \geqslant 0$, the following condition should be satisfied $x_k \leqslant 0.5(x_d + x_m)$. So assuming $\delta^2 = (x_m - x_k)^2$ and $\sigma_r^2 = (x_d - x_k)^2$ implies that the forward and inversion models should on average produce radiance that is equal to or larger than the actual one. This implicit assumption does not reflect the practice of model inversion. Equation (11) may under- or overestimate the observed radi-

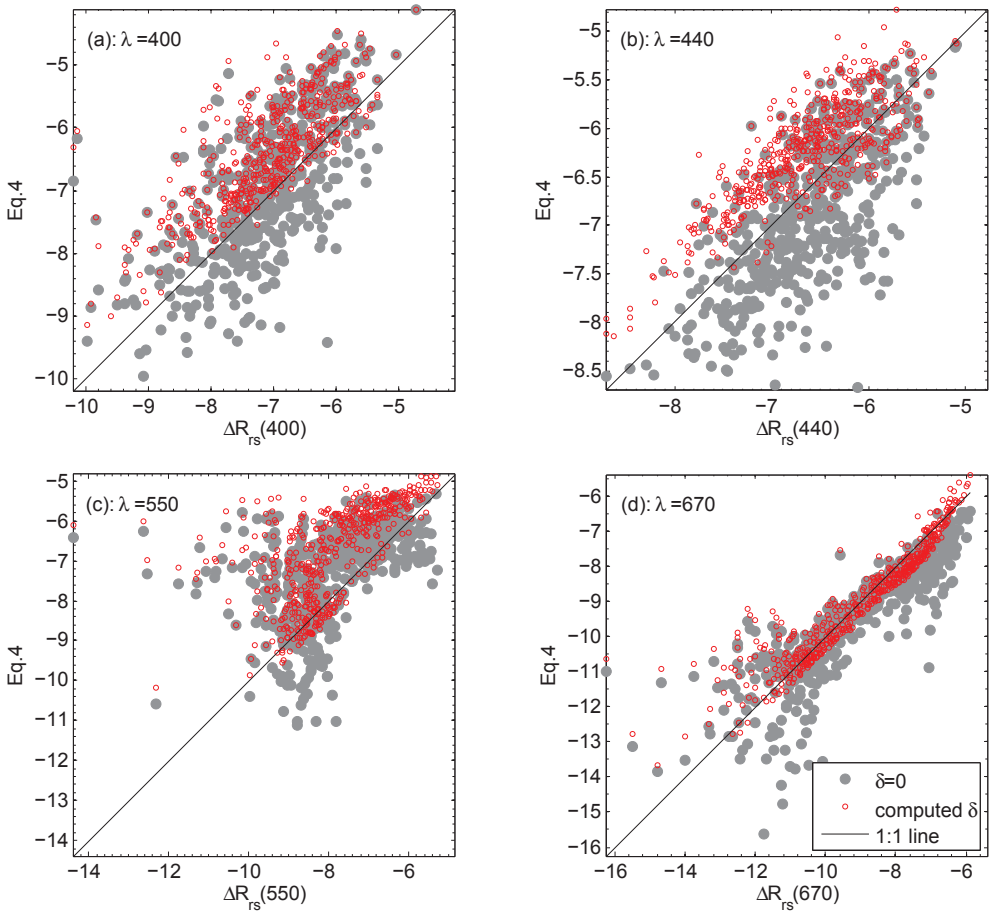

Fig. 2. Comparison between known and estimated radiometric uncertainty for different wavelengths: (a) 400 nm, (b) 440 nm, (c) 550 nm, and (d) 670 nm. The values are log transformed.

#146504 - $15.00 USD Received 25 Apr 2011; revised 4 Jul 2011; accepted 2 Aug 2011; published 15 Aug 2011

ance based on noise level and water contents of dissolved and suspended matters. We avoid, however, this implication by using absolute values, such as $\delta = |x_m - x_k|$ and $\sigma_r = |x_d - x_k|$, which prohibits expanding δ^2 and σ_r^2, and yet guarantees positive value.

Table 2. Goodness-of-Fit Parameters Between Known and Derived Radiometric Uncertainty as Retrieved from IOCCG Data Set

	Eq. (4), $\delta = 0$			Eq. (4), δ computed		
Wavelength nm	MADi	R^2	RMSE	MADi	R^2	RMSE
440	0.695	0.464	0.868	0.443	0.610	0.926
490	0.463	0.531	0.598	0.260	0.664	0.549
560	0.891	0.235	1.381	0.779	0.361	1.564
670	0.529	0.770	0.938	0.376	0.890	0.622

5.2. Validation Results

The ensemble uncertainty, Ψ in Eq. (6), is a function of the weights, w_i, which are obtained from the partial derivatives of $Rs_w(\lambda) = f(\mathbf{iop})$ with respect to IOPs. The weight w_i is only a function of IOPs and Ψ (uncertainty per radiometric error) is nearly independent of the error on Rs_w. As such, Ψ computed for the three data sets should be comparable for similar IOPs, which is confirmed in Fig. 3. For validation, we express the uncertainty in terms of IOPs, which is done by multiplying Ψ by σ_r for the derived error, and by expressing the known error as a sum of weighted IOPs's errors, Eq. (12). The reason behind this weighting is that the ensemble uncertainty of IOPs is also a weighted sum.

The term Δiop_i^2 in Eq. (12) includes the uncertainties associated with $Rs_w(\lambda)$ (for NOMAD and SeaWiFS-matchup), so that the error will increase as the input spectra might have their spectral shapes affected by errors from various sources (sensor noise, atmospheric correction and spatial scale differences). For the SeaWiFS sensor, and the same model-parametrization setup as used in this paper, residuals from atmospheric correction and sensor noise are on average 50% of the total error [8, their Table 2]. The discrepancy in the spatial scale accounts for about 20% of the total error [21, 22]. Thus, the effect of the model-parametrization setup contributes for 30% of the total uncertainty in the derived IOPs. On the other hand, the sensor noise signal in the NOMAD data set contributes by an average of 20% to the total error on derived IOP [8, their Table 4], Moreover, the NOMAD data are affected by surface reflectance, which can be in the same order of magnitude of water signal in case-1 waters [25]. This leaves about 40% of the total error to model-parametrization setup. Two additional error components will be added due to approximating σ_i^2 by Δiop_i^2, and truncating the covariance terms in the Taylor expansion, ℓ in Eq. (4). These reasons could explain the large discrepancy shown in Fig. 1 between known and derived values for the NOMAD and SeaWiFS-matchup data sets.

5.3. Optimum Accuracy of Model-Parametrization Setup

Application of a gradient-based method for estimating the uncertainties in derived IOPs produces values proportional to the magnitude of IOPs and radiometric uncertainty [6,8]. This proportionality is compensated for by normalizing Ψ to the sum of derived IOPs, $\Psi^N(\lambda)$. Doing so will result in a measure of relative ensemble uncertainty per unit error of radiance. However, for most of the ocean waters, where $a \gg b_b$, the sum of IOPs (cb) is equivalent to the total absorption coefficient, which makes cb hard to interpret statistically. The reciprocal of $\Psi^N(\lambda)$ is the radiometric uncertainty normalized to the relative ensemble error, $\sigma_r^N(\lambda)$. The normalized radiometric uncertainty, σ_r^N, is expected to increase with water load of dissolved and suspended

#146504 - $15.00 USD Received 25 Apr 2011; revised 4 Jul 2011; accepted 2 Aug 2011; published 15 Aug 2011

matters (turbidity), and approaches a constant value for waters with a high turbidity. Figure 3 shows σ_r^N, computed from derived values, versus the sum of known IOPs, cb_k.

For the three data sets, the normalized radiometric uncertainty approaches a constant value for $cb_k(440) \geq 0.4$ m^{-1}, with σ_r^N of about 0.0783 sr^{-1} (-2.547 on the log scale). This value, 0.0783, is very high and close to the saturation-of-reflectance (SoR) of the employed ocean color model, i.e. Eq. (11), SoR is defined here as being the highest radiometric value that can be produced by the ocean color model. This situation occurs in waters loaded with non-absorbing particles such that the fraction u in Eq. (11) approaches unity (i.e. absorption by constituents is small in comparison to backscattering $b_b \gg a$). In this case, SoR $= \lim_{u\to 1} \mathrm{Rs_w} = 0.0922$ sr^{-1}. Conversely, the reciprocal of $\sigma_r^N(\lambda)$, Ψ_λ^N, decreases with increasing water turbidity reaching a constant value of $1/0.0922 = 10.85$ sr. It is clear from the above discussion that higher radiometric uncertainty ($\sigma_r^N(\lambda)$) is expected for turbid waters, and the relative ensemble uncertainty is expected to be higher for clear water. In addition, Fig. 3 allows us also to provide an estimate of the optimum accuracy that is achievable with a model-parametrization setup. The maximum value of normalized radiometric uncertainty (at 440 nm) is computed as 0.0783 sr. This value can be converted to ensemble uncertainty using $cb_k(440) \approx 0.4$ m^{-1} as: $0.4/0.0783 = 5.11$ sr m^{-1}. The minimum value of normalized radiometric uncertainty (also at 440 nm, see Fig. 3) is 0.0369 sr which corresponds to $cb_k(440) \approx 0.0123$ m^{-1}. In the same way we compute the minimum value of ensemble uncertainty as: $0.0123/0.0369 = 0.33$ sr m^{-1}. The lower limit of the ensemble uncertainty shows that the ocean color model and IOPs parameterizations have an inherent error at 440 nm of at least 0.333 sr m^{-1}. Therefore, each error of 1 sr^{-1} results in 0.33 m^{-1} collective error of IOPs. This lower limit of error represents the optimum (maximum) accuracy that can be achieved by a model-parametrization setup.

Nominal values for radiometric error at 440 nm are in the range of 0.0024 sr^{-1} (for IOCCG)

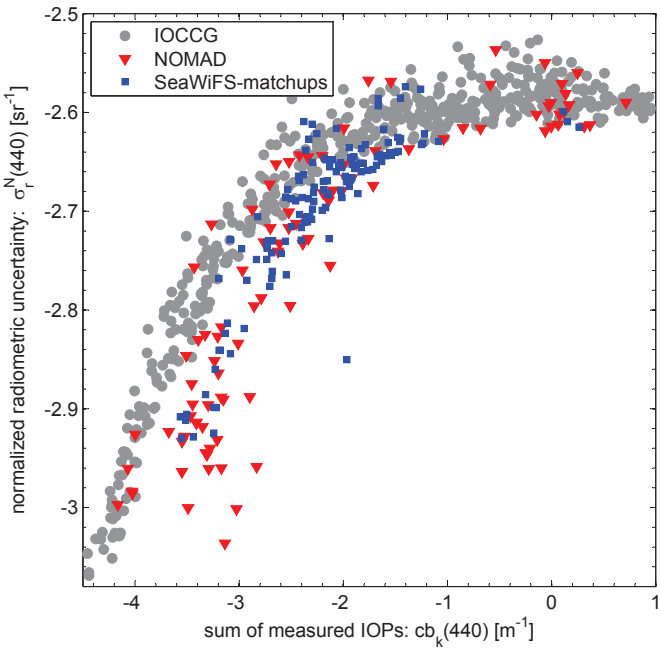

Fig. 3. The relationship between the normalized radiometric uncertainty, σ_r^N, and the sum of known IOPs values, cb_k. The values are log transformed.

#146504 - $15.00 USD Received 25 Apr 2011; revised 4 Jul 2011; accepted 2 Aug 2011; published 15 Aug 2011

and 0.0050 sr^{-1} (for NOMAD and SeaWiFS-matchup). These values are derived as the difference between model best-fit and observed remote reflectance, and averaged for each data set. In consequence, the highest (optimum) accuracy of the used model-parametrization setup is $\Delta cb(440) = 0.0024 \times 0.33 = 0.0008$ m^{-1} for IOCCG and $\Delta cb(440) = 0.005 \times 0.33 = 0.0017$ m^{-1} for NOMAD and SeaWiFS-matchup. These values increase to their maxima for SoR (using the value 5.11 sr m^{-1}) of 0.0123 m^{-1} and 0.0256 m^{-1}, respectively.

5.4. Global product of the ensemble uncertainty

As a demonstration of the benefit of the developed method for quantifying uncertainties in existing products, Eq. (6), is applied to monthly mean values of GSM-derived IOPs from 1997-2007, and per year. From the annual mean ensemble uncertainty, the trend is computed using a linear regression model, which is shown in Fig. 4. Several areas (e.g., northern part of the Black Sea and the Caspian sea, Baltic Sea, Okhotsk Sea, Bohai Sea, Gulf of St.Lawrence etc) can be identified as regions with increasing trends up to 8 sr m^{-1}decade^{-1}. Using an average radiometric error of 0.005 sr^{-1} (obtained from the SeaWiFS-matchup data), this value is equivalent to a $\Delta cb(440)$ of 0.04 m^{-1}decade^{-1}. Via this application of our method, it is shown that the GSM model-parametrization setup produces IOPs subject to an increasing level of uncertainty in specific regions. As such, the method has the potential of detecting areas for which the model-parametrization setup should be considered. Moreover it provides also a means to identify changes in the biophysical characteristics of waters associated to, for example, changes in climate or anthropogenic influences.

Analyzing the spatial distribution of $\Psi^{N}(440)$ annual values (not shown here) show persistent patterns of high values of $\Psi^{N}(440)$ throughout the last decade in the subtropical gyres, whereas lower values are observed in most coastal areas. Moreover, the spatial distribution of the relative ensemble uncertainty largely resembles the observed values of remote sensing reflectance at 443 nm. These results can also be deduced from Fig. 3 and are in accordance with the global uncertainty maps for Chlorophyll-a by Mélin [2] for the subtropical gyres, whereas, the global distribution of $\Psi(440)$, see Eq.(9), corresponds to the results of Moore *et al.* [3] (see their Fig. 5).

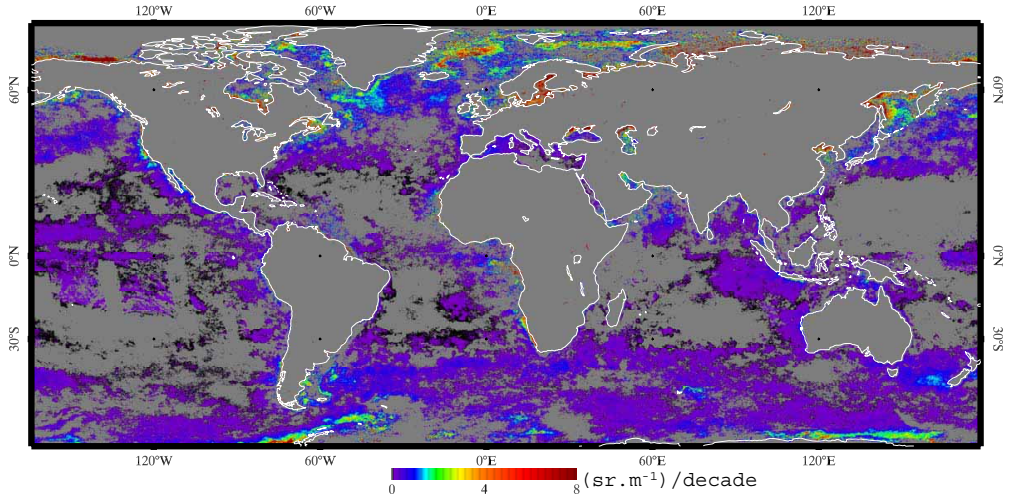

Fig. 4. Trends of ensemble uncertainty at 440 nm between the period 1997-2007.

#146504 - $15.00 USD Received 25 Apr 2011; revised 4 Jul 2011; accepted 2 Aug 2011; published 15 Aug 2011

6. Conclusions

A method is presented for the quantification of the combined accuracy of ocean color models and the parameterizations of inherent optical proprieties (IOPs), or model-parametrization setup. Its application produces a single (or ensemble) uncertainty measure for the collective errors in the derived IOPs relative to the radiometric uncertainty without the need for model inversion or prior information on the radiometric errors. As such, the method is directly applicable to existing satellite based IOP products. It can be used to compare different satellite data products and in a context of data merging where the respective uncertainties associated with the input data streams are required.

A thorough validation of the method is presented using simulated, *in-situ* measured and ocean color matchup data. For the synthetic data a very good fit is obtained between the derived and known values ($R^2 > 0.95$ and mean absolute difference (MADi) < 0.25 m^{-1}). A reduced performance ($0.45 < R^2 < 0.5$ and $0.65 <$ MADi < 0.9) is, however, found for the *in-situ* and ocean color matchup data, which is attributed to additional error sources such as sensor noise, atmospheric correction and spatial scale differences. Further, we employ the method also for estimating optimum accuracy that could be achieved with the three data sets for a specific model-parametrization setup, which could be seen as the target accuracy in retrieving IOPs.

Application to time series (1997-2007) of global IOP products illustrates the capability of the method in identifying areas subject to large uncertainties. Specifically, the analysis of the annual trend reveals regions with ensemble uncertainties increasing at rates up to 8.0 sr m^{-1} decade^{-1}. Such trends are likely related to changes in the biophysical characteristics of waters associated with, for example, climatic changes or anthropogenic influences.

Quantifying the ensemble uncertainty of IOPs provides the optimum accuracy which can be achieved by a model-parametrization setup. Moreover, it has the potential of detecting areas for which the performance of a given model-parametrization setup is suboptimal or deteriorating. This provides the information needed for updating the global model-parametrization setup, which contributes to the overall uncertainty reduction within IOP products.

Acknowledgments

The authors would like to thank NASA Ocean Biology Processing Group and individual data contributors for maintaining and updating the SeaBASS database and the NASA Goddard Earth Sciences Data and Information Services Center for providing Giovanni online data system. SeaWiFS and MODIS missions scientists and associated NASA personnel are acknowledged for the production of the data used in this paper. Three anonymous referees are acknowledged for reviewing the manuscript.

#146504 - $15.00 USD Received 25 Apr 2011; revised 4 Jul 2011; accepted 2 Aug 2011; published 15 Aug 2011